Heave Compensation Control of Drill String System Based on Single Neuron PID for Oceanic Drilling

Jing Ren[1,2,3], Chengda Lu[1,2,3,4,†] Chenxuan Wang[1,2,3], Zhejiaqi Ma[2,3,4], Chao Gan[1,2,3,4], Fulong Ning[1,3,5], and Min Wu[1,2,3,4]

[1] School of Future Technology, China University of Geosciences, Wuhan 430074, China
[2] Hubei Key Laboratory of Advanced Control and Intelligent Automation for Complex Systems, Wuhan 430074, China
[3] Engineering Research Center of Intelligent Technology for Geo-Exploration, Ministry of Education, Wuhan 430074, China
[4] School of Automation, China University of Geosciences, Wuhan 430074, China
[5] Faculty of Engineering, China University of Geosciences, Wuhan 430074, China

Abstract. During offshore exploration operations, vessels are subjected to six degrees of freedom motion due to the influence of wind, waves, and currents. Among these motions, heave is particularly challenging to compensate for and can significantly impact the drilling process. This paper designs an active heave compensation control for the drill string system used in offshore exploration. It addresses the issue of parameter uncertainty by developing a single neuron PID control method based on a quadratic performance index. Simulation analysis is conducted in the MATLAB environment. The simulation results, when compared to other controllers, show that the proposed controller produces smooth outputs, verifying its effectiveness in compensation and its ability to overcome the limitations of conventional PID controllers.

Keywords: Active Heave Compensation · Single Neuron PID · Ocean Drilling · Deep-Sea Resource Exploration.

1 Introduction

Since 1940, with the advancement of technology and the continuous depletion of terrestrial resources, humanity has turned its gaze toward the ocean [1]. In response to energy shortages, nations are gradually shifting their focus on marine resource development from shallow coastal areas to the sea depths. The exploitation of deep-sea resources has thus become a pivotal component of national development strategies worldwide.

During marine exploration, vessels undergo six degrees of freedom motion, including sway, heave, roll, pitch, yaw, and surge, influenced by waves, currents,

† Corresponding author: Chengda Lu (luchengda@cug.edu.cn).

and sea winds. These movements subsequently affect the vertical motion of marine resource exploration platforms. Typically, a dynamic positioning system can mitigate horizontal motion [2], but it cannot compensate for the heave motion of the platform. This leads to significant fluctuations in suspension tension, impacting drilling bit penetration and efficiency, and may even result in accidents such as drill string bottoming incidents. Hence, research into heave compensation devices is warranted. There are generally two types of heave compensation methods: Active Heave Compensation (AHC) and Passive Heave Compensation (PHC). PHC is a follow-up compensation method, where it is challenging to improve compensation efficiency [3]. In contrast, AHC, with additional energy input, offers high compensation accuracy and fast response speed. Currently, various control strategies have been proposed by scholars for AHC, such as Model Predictive Control (MPC) [4], adaptive control based on backstepping [5], and fuzzy PID methods.

Hydraulic drive systems are commonly utilized in active heave compensation systems [6]. Due to the influence of working conditions, hydraulic system parameters or load parameters may exhibit specific perturbations under different operating conditions. For instance, changes in temperature and component wear can lead to fluctuations in hydraulic parameters, resulting in system instability or reduced compensation accuracy [7]. Therefore, the designed controller should possess strong adaptive capabilities.

Traditional PID control is commonly used and requires proper parameter selection. Parameter tuning methods, such as the relay feedback method and the critical gain method, can easily induce system oscillations [8]. Additionally, once set, the parameters cannot be modified in real-time according to system characteristics, resulting in suboptimal control performance. When considering the integration of neural networks with PID, using a multilayer neural network as an adaptive controller involves adjusting numerous weight coefficients, resulting in slow responsiveness during real-time adjustments.

This paper designed an adaptive single-neuron PID controller utilizing an incremental PID structure. This controller is similar to a traditional PID controller but incorporates a neural network for online adjustment of the PID parameters. This adaptive tuning enables the controller to dynamically adjust to the system's changing characteristics, effectively responding to parameter variations and external disturbances. Consequently, it enhances the compensation control for the heave motion of the drill string system in marine exploration.

2 Process Characteristics Analysis and Control System Structure

First, a brief overview of the drilling process considering the heave compensation system is provided. By analyzing this process, the control objectives of this study are identified, and a dynamic model of the system is developed. This model serves as the foundation for the subsequent simulation experiments.

2.1 Process Description and Characteristics Analysis

The heave compensation system is installed between the traveling block and the hook [9, 10], as depicted in **Fig. 1**. During drilling, the equilibrium relationship between the drill string suspended on the hook, the downhole drilling pressure, and the compensating hydraulic cylinder is

$$2P_L A_P + W - Q = 0, \tag{1}$$

where P_L is the hydraulic pressure in the cylinder, A_P is the piston area in the compensating device cylinder, Q is the total weight of the drill string suspended on the hook, and W is the downhole drilling pressure.

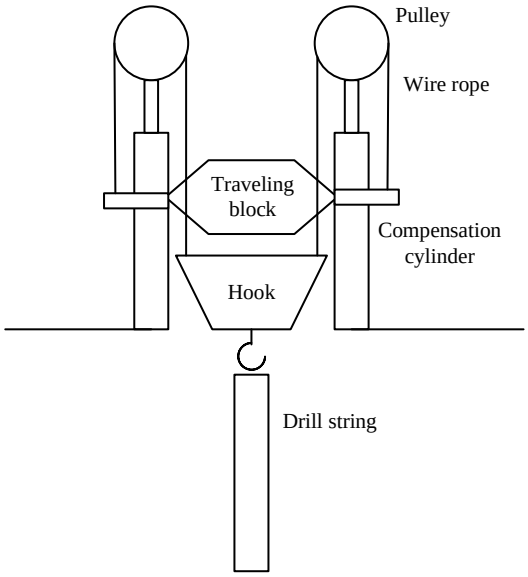

Fig. 1. The structure of heave compensation and drill string system.

As indicated by Eq.(1), adjusting the pressure in the hydraulic cylinder can alter the drilling pressure. During offshore exploration operations, where heave motion affects drilling pressure, maintaining stable drilling pressure only requires the supply of hydraulic oil to the cylinder's oil chamber, thereby causing the piston to move and achieving the desired compensation effect [11].

Assuming a simplified drill string model composed of drill pipes, drill collars, and drill bits, variations in drilling pressure cause changes in the lengths of the drill string and drill collars. The changes can be calculated separately according to Hooke's Law

$$\begin{aligned} \Delta L_1 &= \frac{\Delta N L_1}{E A_1}, \\ \Delta L_2 &= \frac{\Delta N L_2}{E A_2}, \end{aligned} \tag{2}$$

where L_1 and L_2 are the lengths of the drill pipe and the drill collar, respectively. ΔN is the change in drilling pressure, E is the elastic modulus of the drill string. A_1 and A_2 are the cross-sectional areas of the drill pipe and the drill collar.

From Eq.(2), the sum of the changes in length can be regarded as the displacement of the hook due to heave motion. Therefore, the control objective can be shifted from stabilizing drilling pressure to controlling the displacement of the hook within a certain range.

2.2 Dynamic Model of Heave Compensation System

Performing a dynamic analysis of the drilling process involves treating one-third of the total mass of the drill string as its equivalent mass, which, along with the spring, acts as the tension applied to the bottom of the drill string. The tension on the drill string is simplified as a spring-mass-damper system. Components such as the heave compensation device, traveling block, and hook are considered rigid bodies, while the piston and lower frame are regarded as a mass M_c at the top of the drill string. The fluid in the compensating cylinder and the gas in the accumulator are treated as weightless springs with an elastic coefficient k_1, and their fluid viscosity coefficient is denoted as c_1 [12].

The heave displacement of the vessel is denoted as x_t , and the displacements of the piston and hook are denoted as x_p , x_h. Referring to **Fig. 2**, based on Newton's second law, the equations of motion for the piston and hook can be established as

$$\begin{aligned} M_c\ddot{x}_p &= k_1(x_p - x_t) + c_1(\dot{x}_p - \dot{x}_t) - F_2, \\ M_d\ddot{x}_h &= -k_d x_h - c_2\dot{x}_h + F_2, \end{aligned} \tag{3}$$

where M_d is the equivalent mass of the drill string. F_2 is the force exerted by the wire rope on the piston, which is equal in magnitude but opposite in direction to the force exerted by the wire rope on the piston. c_2 is the viscous drag coefficient of the drill string in the mud. k_d is the equivalent stiffness of the drill string, which can be calculated as

$$k_d = \frac{\Delta N}{\Delta L_1 + \Delta L_2}. \tag{4}$$

The relative displacement of the compensation cylinder piston relative to the cylinder body is denoted as x_b. Due to the effect of the pulley's pitch radius, the relationship between x_h and x_p is as

$$\begin{aligned} x_h &= 2x_p - x_t, \\ x_b &= \frac{1}{2}(x_h - x_t). \end{aligned} \tag{5}$$

By inputting hydraulic oil to control the compensation cylinder piston, the continuity equation for the input of hydraulic oil into the compensating hydraulic cylinder is

$$q_L = A_p\dot{x}_b, \tag{6}$$

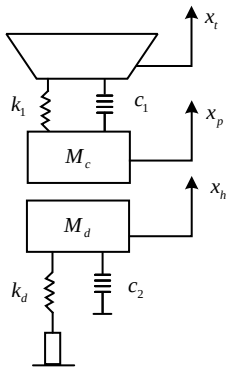

Fig. 2. Heave compensation device and drill string dynamic analysis diagram.

where A_p is the area of the compensation cylinder piston.

By combining Eqs.(3)-(6), the output y is defined as the hook displacement, $y = x_h$, and the input u is defined as the hydraulic flow rate, $u = q_L$. The system's differential equation is established as

$$\begin{aligned} &\dddot{y} + \frac{c_2}{M_c + 2M_d}\ddot{y} + \frac{k_d}{M_c + 2M_d}\dot{y} = \\ &\frac{1}{A_p}\ddot{u} + \frac{c_1}{A_p(M_c + 2M_d)}\dot{u} + \frac{k_1}{A_p(M_c + 2M_d)}u, \end{aligned} \tag{7}$$

selecting the state variables as

$$X = \begin{bmatrix} x_1 \\ x_2 \\ x_3 \end{bmatrix} = \begin{bmatrix} y \\ \dot{x}_1 - \dfrac{1}{A_p}u \\ \dot{x}_2 - \dfrac{c_1 - c_2}{A_p(M_c + 2M_d)} \end{bmatrix}. \tag{8}$$

Thus, the state-space representation of the flow-rate to the hook system is formulated as

$$\begin{aligned} \dot{X} = &\begin{bmatrix} 0 & 1 & 0 \\ 0 & 0 & 1 \\ 0 & \dfrac{-k_d}{M_c + 2M_d} & \dfrac{-c_2}{M_c + 2M_d} \end{bmatrix} X + \\ &\begin{bmatrix} \dfrac{1}{A_p} \\ \dfrac{c_1 - c_2}{A_p(M_c + 2M_d)} \\ \dfrac{(M_c + 2M_d)(k_1 - k_d) - c_2(c_1 - c_2)}{A_p(M_c + 2M_d)^2} \end{bmatrix} u, \\ y = &\begin{bmatrix} 1 & 0 & 0 \end{bmatrix} X. \end{aligned} \tag{9}$$

3 Design of Heave Compensation Control

This section presents the design of a displacement compensation system based on the analysis above. First, the components of the control loop, including the controller, variable pump, and heave compensation cylinder, are briefly described. Then, a single-neuron PID controller is designed based on quadratic performance criteria.

3.1 Control Loop

The heave compensation system injects hydraulic oil into the compensation cylinder in real-time by detecting the displacement of the hook, thereby compelling piston movement to maintain positional equilibrium. The control system block diagram is shown in **Fig. 3**.

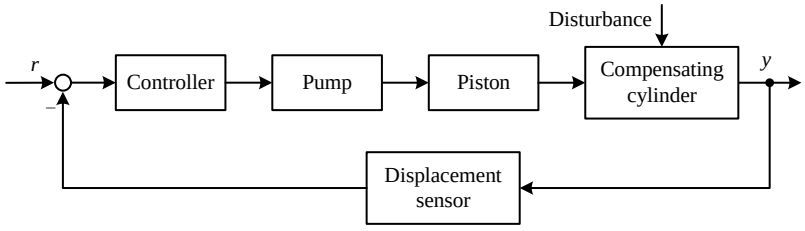

Fig. 3. Block diagram of active heave compensation system.

The heave motion of the vessel in waves can be represented as a synthesis of a series of sine waves. The wave equation from reference [13] is adopted as the simulated heave motion of the vessel and is given as

$$\begin{aligned} x_t(t) = -\,[&0.5\sin(2\pi \times 0.1t) + 0.6\sin(2\pi \times 0.08t) \\ &+ 0.3\sin(2\pi \times 0.075t) + \sin(2\pi \times 0.07t)]. \end{aligned} \tag{10}$$

The heave motion signal of the vessel described above is inverted and then used as the reference $r = -x_t$ to the controller. The controller commands the hook, controlled by the heave compensation system, to track the desired trajectory, thereby offsetting the heave motion of the vessel.

3.2 Control Design

A typical incremental PID structure is as

$$\Delta u = K_p(e(k) - e(k-1)) + K_I e(k) + K_D(e(k) - 2e(k-1) + e(k-2)), \tag{11}$$

where k is the sampling index.

A single neuron PID structure adds a neuron to the traditional PID framework, as illustrated in **Fig. 4**. The reference input r and the system output y are

transformed into three inputs, x_1, x_2, and x_3 of the neuron. The error satisfies $e = r - y$. The proportional, integral, and derivative coefficients are considered as the corresponding weights w_1, w_2, w_3, which are adjusted according to specific learning rules.

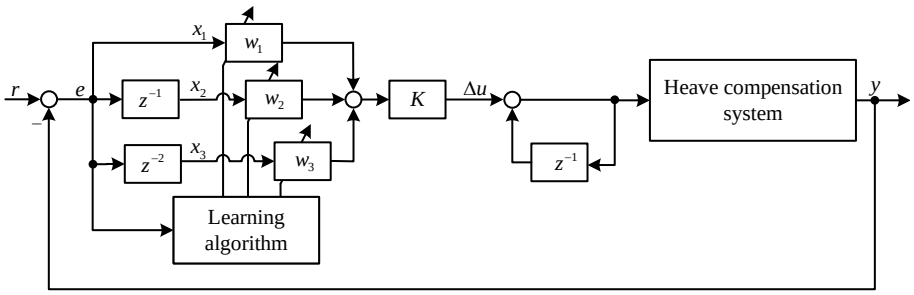

Fig. 4. Single-neuron PID structure diagram.

The PID control increment Δu of the neuron output is

$$\Delta u = K(\sum_{i=1}^{3} w_i(k)x_i(k)), \tag{12}$$

and

$$u(k) = u(k-1) + \Delta u, \tag{13}$$

where K represents the introduced proportional coefficient, corresponding to the learning rate of the single neuron. x_1 is $e(k) - e(k-1)$, x_2 is $e(k)$, and x_3 is $e(k) - 2e(k-1) + e(k-2)$.

Let $w_i'(k) = \dfrac{w_i(k)}{\sum_{i=1}^{3} w_i(k)}$, the equation is then rewritten as

$$\Delta u = K(\sum_{i=1}^{3} w_i'(k)x_i(k)). \tag{14}$$

The supervised Hebbian learning rule [14] facilitates adaptive control by dynamically adjusting the weighting coefficients through modification of the three PID parameters in response to real-time deviations. Specifically, each weight is updated proportionally to both the output error $e(k)$ and the corresponding input signal, enabling real-time tuning of the PID parameters to optimize system performance. The learning process using the supervised Hebbian learning rule is

$$\begin{cases} w_1(k) = w_1(k-1) + \eta_P e(k)u(k)x_1(k), \\ w_2(k) = w_2(k-1) + \eta_I e(k)u(k)x_2(k), \\ w_3(k) = w_3(k-1) + \eta_D e(k)u(k)x_3(k), \end{cases} \tag{15}$$

where η_P, η_I, η_D and represent the learning rates of the three PID parameters, respectively.

To achieve smoother output from the controller, this study borrows from the idea of a quadratic performance index in optimal control to achieve smoother output from the controller. According to linear quadratic optimal control theory [15], the weight coefficients of the single-neuron PID controller are adjusted based on the minimization of the weighted sum of squares of output error and control increment, indirectly enforcing constraint control on the weighted output error and control increment. Let P and Q represent the weighting coefficients for the output error and control increment, respectively. The performance index is defined as

$$J(k) = \frac{1}{2}(P(r(k) - y(k))^2 + Q\Delta^2 u(k)). \tag{16}$$

According to the gradient descent method, the adjustment of $w_i(k)$ in the direction of reducing J is given by

$$\begin{aligned} \Delta w_i(k) &= w_i(k) - w_i(k-1) = -\eta_i \frac{\partial J(k)}{\partial w_i(k)}, \\ \frac{\partial J(k)}{\partial w_i(k)} &= K x_i(k)[-Pe(k)\frac{\partial y(k)}{\partial u(k)} + QK\sum_{i=1}^{3} w_i(k)x_i(k)], \end{aligned} \tag{17}$$

where $\frac{\partial y(k)}{\partial u(k)}$ is replaced by the first value of the output obtained by adding a unit step to the input at zero initial states, denoted as b_0. In summary, the learning algorithm for the single-neuron PID controller based on quadratic performance indicators is

$$\begin{aligned} u(k) &= u(k-1) + K(\sum_{i=1}^{3} w'_i(k)x_i(k)), \\ w'_i(k) &= \frac{w_i(k)}{\sum_{i=1}^{3} w_i(k)}, \\ w_i(k) &= w_i(k-1) + \eta_i K\{Pb_0 e(k)x_i(k) \\ &\quad - QK\sum_{i=1}^{3}[w_i(k)x_i(k)]x_i(k)\}. \end{aligned} \tag{18}$$

4 Simulation Validation

To verify the feasibility and effectiveness of the proposed method, this section simulates the aforementioned drill string heave compensation system using MATLAB/Simulink. It compares the control performance of a single neuron PID controller based on a quadratic performance index, a single neuron PID controller based on the supervised Hebb learning rule, and a conventional PID controller.

4.1 Simulation Design

The input for all controllers was the desired compensatory motion, with the output being the hydraulic oil flow rate. The initial parameters of the system and the controller parameters were provided in **Table 1**.

Table 1. System and the controller parameters.

-	M_c	M_d	c_1	c_2	k_1	k_d	η_P	η_I	η_D	K	P	Q
Values	25	100	1639	1-1.5	72.1	90249	25	10	5	0.6	20	0.5
Unites	t	t	Ns/m	-	MPa	N/m	-	-	-	-	-	-

In the model illustrated in Section 2.2, the true values of parameters such as c_1, c_2, k_1, and k_d were subject to uncertainty, and there could have been parameter perturbations under different operating conditions. To verify the ability of the single-neuron PID controller to maintain stable output under parameter variations, the changing parameters were assumed to be c_2 and k_d. Here, c_2 was randomly selected between 1 and 1.15, and k_d was initially fixed for the first 50 seconds and then increased by 10 N/m every 10 seconds starting from the 50th second. Meanwhile, the system was subjected to unknown disturbances after fixing the controller parameters. During simulation, a sine signal was introduced starting from the 55th second to observe and compare the system response and control performance using different controllers under parameter variations and disturbances conditions.

4.2 Simulation Results and Analysis

The simulation results, depicted in **Fig. 5** - **Fig. 7**, compared the tracking performance of three different controllers. These included a single-neuron PID controller designed using a quadratic performance index (red line, Our method), a single-neuron PID controller based on a supervised Hebbian learning rule (blue line, Hebb), and the conventional PID controller (yellow line, PID). The dynamic performance and stability of the system's step response were analyzed to select the optimal parameters for the conventional PID controller. The black curve in **Fig. 5** represented the desired compensation trajectory.

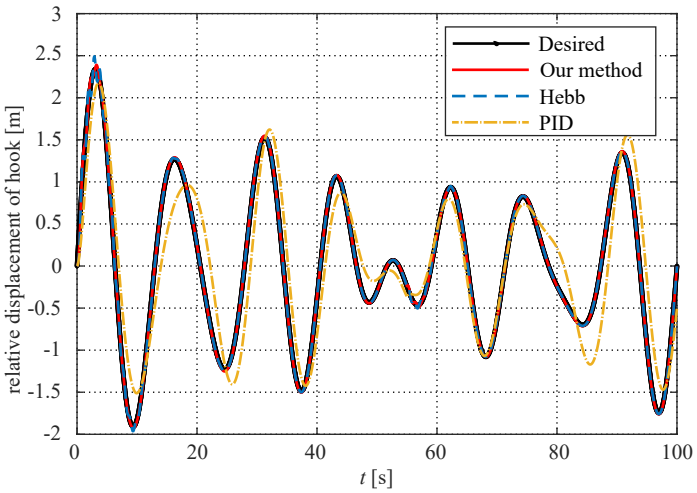

Fig. 5. Tracking results under different controllers.

From **Fig. 5**, it can be observed that the tracking compensation effect of the single-neuron PID was significantly superior to the conventional PID, showing faster response speed and better tracking performance. Even when the model parameters change at 50 seconds, it still maintained good tracking performance, and there was no significant change after the introduction of disturbance at 55 seconds. As stated in Section 2.3, the compensation target of the system in this paper was to control the actual heave displacement of the hook so that it did not to exceed $\Delta L_1 + \Delta L_2$, which was 97.73 mm. Therefore, it was necessary to calculate the actual displacement of the hook, which was the difference between the hook displacement and the compensation signal.

Fig. 6 depicted the actual displacement of the hook under the influence of different controllers, providing insights into the compensation effectiveness. When the heave motion reached its maximum value of 2342 mm with a range of ±5%, the compensation error of the quadratic algorithm controller was contained within 60.60 mm, achieving a compensation rate of 93.18%. On the other hand, the compensation error for the conventional single-neuron algorithm controller ranged within 169.7 mm, while the maximum compensation error for the conventional PID controller of the hook reached 398.7mm. Neither of these approaches satisfied the requirement of keeping the hook displacement within 97.73 mm.

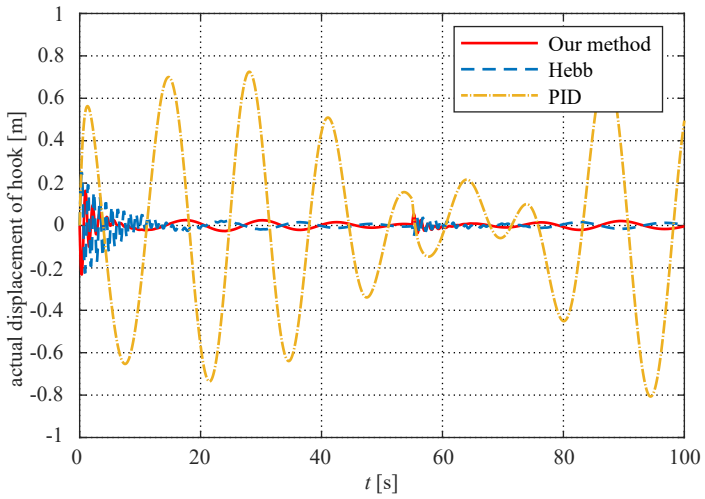

Fig. 6. Actual heave displacement of the hook for different controllers.

Table 2. presented the overall Root Mean Square Error (RMSE) of hook displacement for various controllers. Additionally, it detailed the RMSE and the maximum error occurring when the heave motion reached its peak value of 2342 mm within a ±5% range.

Fig. 7 illustrated the controller outputs of the quadratic algorithm and the conventional single-neuron algorithm. A comparison between the two revealed that the quadratic algorithm, incorporating a minimization of control increments

Table 2. Error comparison under different controllers.

Controller	RMSE	RMSE(%5)	Max error(%5)
Quadratic	22.90	37.00	60.60
Hebb	32.60	100.5	169.7
PID	394.9	252.3	398.7

in its weight adjustment rule, generated smoother control actions for the PID controller, thereby enhancing control stability.

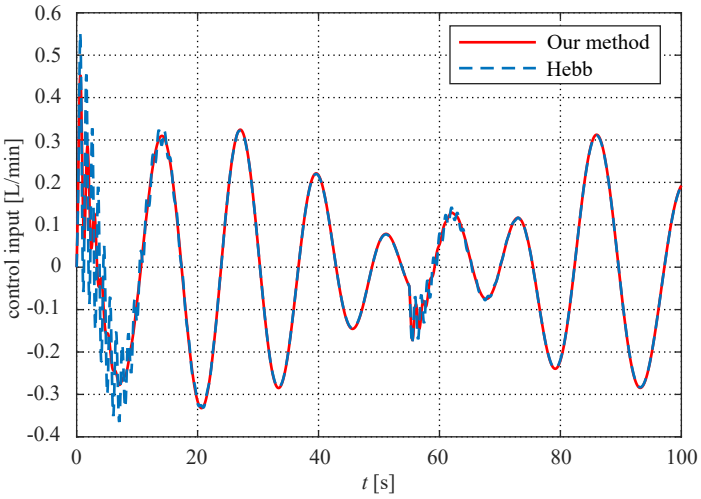

Fig. 7. Output results for different single-neuron controllers.

5 Conclusion

To address the issues of random disturbances and parameter uncertainties in the heave compensation control of the drill string system, this paper investigates a single-neuron PID controller employing a quadratic performance index, enabling real-time adjustment and automatic tuning of PID parameters. Simulation results demonstrate that, in the presence of disturbances and parameter variations, the controller based on the quadratic algorithm exhibits rapid and automatic recovery to a stable tracking state after initial oscillations. Moreover, the average fluctuations conform to the drilling pressure requirements outlined earlier, showcasing excellent dynamic performance. Compared to conventional single-neuron and PID controllers, the quadratic algorithm achieves superior control effects, meeting the active heave compensation needs of the drill string system.

Acknowledgements This paper is supported by the National Natural Science Foundation of China under Grant 62333019, the 111 project under Grant B17040, the Fundamental Research Funds for the Central Universities, China University of Geosciences.

References

1. He, Q., Wang, P.: Current Situation and Prospect of Deep-Sea Energy Development. Ocean Development and Management **34**(12), 66–71 (2017)
2. Ma, L., Wang, Y., Han, Q.: Event-triggered dynamic positioning for mass-switched unmanned marine vehicles in network environments. IEEE Transactions on Cybernetics **52**(5), 3159–3171 (2020)
3. Sánchez, W.H.C., Fortaleza, E.L.F., Neto, A.B., et al.: Effects of nonlinear friction of passive heave compensator on drilling operationPart II: Active robust control. Ocean Engineering **227**, 108837 (2021)
4. Woodacre, J., Bauer, R., Irani, R.: Hydraulic valve-based active-heave compensation using a model-predictive controller with non-linear valve compensations. Ocean Engineering **152**, 47–56 (2018)
5. Ahn, K.-K., Nam, D.-N.-C., Jin, M.: Adaptive Backstepping Control of an Electrohydraulic Actuator. IEEE/ASME Transactions on Mechatronics **19**(3), 987–995 (2014).
6. Woodacre, J.-K., Bauer, R.-J., Irani, R.-A.: A review of vertical motion heave compensation systems. Ocean Engineering **104**, 140–154 (2015)
7. Helian, B., Zheng, C., Yao, B.: Energy-saving and accurate motion control of a hydraulic actuator with uncertain negative loads. Chinese Journal of Aeronautics **34**(5), 253–264 (2021)
8. Hao, J., Zhang, G., Liu, W., Zheng, Y., Ren, L.: Data-Driven Tracking Control Based on LM and PID Neural Network With Relay Feedback for Discrete Nonlinear Systems. IEEE Transactions on Industrial Electronics **68**(11), 11587–11597 (2021)
9. Lei, J., Li, H., Tang, W., Tian, Y., Yang, Q., Cao, S.: AMESim-based Study on Control Method and Simulation of Drill String Compensation System. Chinese Hydraulics & Pneumatics **0**(10), 83 (2019)
10. Sánchez, W.H.C., Neto, A.B., Fortaleza, E.L.F.: Effects of nonlinear friction of passive heave compensator on drilling operationPart I: Modeling and analysis. Ocean Engineering **213**, 107743 (2020)
11. Xu, J., Yi, B., Zhan, Y.: Review of Heave Compensation Systems: Design and Control Strategies. In: 2023 IEEE 11th International Conference on Computer Science and Network Technology (ICCSNT), pp. 406–413. IEEE (2023). https://doi.org/10.1109/ICCSNT58790.2023.10334591
12. Xu, T., Liu, Q., Dai, J., Li, W.: Design and simulation analysis of new semi-active and multiplication process heave compensation device. China Mechanical Engineering **27**(5), 663 (2016)
13. Li, H., Fu, J., Fan, S., Chen, T., Li, P., Zheng, W.: Simulation on Drill String Compensation Device Based on Heave Prediction. China Petroleum Machinery **49**(3), 57–64 (2021)
14. Ding, F., Zhang, W., Luo, X., Hu, L., Zhang, Z., Wang, M., Li, H., Peng, M., Wu, X., Hu, L., Zhang, T.: Gain self-adjusting single neuron PID control method and experiments for longitudinal relative position of harvester and transport vehicle. Computers and Electronics in Agriculture **213**, 108215 (2023)
15. Rezaei, P., Aria, H.P., Ayati, M.: LQR based Optimal Passive Fault-Tolerant Nonlinear Fractional-Order PID. In: 2021 16th International Conference on Engineering of Modern Electric Systems (EMES), pp. 1–4. IEEE (2021). https://doi.org/10.1109/EMES52337.2021.9484123